Open Archive TOULOUSE Archive Ouverte (OATAO)

OATAO is an open access repository that collects the work of Toulouse researchers and makes it freely available over the web where possible.

This is an author-deposited version published in: http://oatao.univ-toulouse.fr/
Eprints ID : 19503

Any correspondence concerning this service should be sent to the repository administrator: staff-oatao@listes-diff.inp-toulouse.fr

Numerical simulation of a periodic circulating fluidized bed of binary mixture of particles: Budget analysis

Solène Chevrier, Pascal Fede, Olivier Simonin,

Institut de Mécanique des Fluides de Toulouse (IMFT) , Université de Toulouse, CNRS, INPT, UPS, Toulouse FRANCE

Abstract

Detailed sensitivity numerical studies have shown that the mesh cell-size may have a drastic effect on the modelling of circulating fluidized bed. Typically the cell-size must be of the order of few particle diameters to predict accurately the dynamical behaviour of a fluidized bed. Then the Euler-Euler numerical simulations of industrial processes are generally performed with grids too coarse to allow the prediction of the local segregation effects. A filtered approach is developed where the unknown terms, called sub-grid contributions, have to be modelled. Highly resolved simulations are used to develop the model. They consist of Euler-Euler simulations with grid refinement up to reach a mesh independent solution. Then spatial filters can be applied in order to measure each sub-grid contribution appearing in the theoretical filtered approach. Such kind of numerical simulation is very expensive and is restricted to very simple configurations. In the present study, highly resolved simulations are performed to investigate the sub-grid contributions in case of a binary particle mixture in a periodic circulating gas-solid fluidized bed. A budget analysis is carried out in order to understand and model the effect of sub-grid contribution on the hydrodynamic of polydisperse gas-solid circulating fluidized bed.

Keywords: gas-solid flow, circulating fluidized bed, polydisperse mixture, filtered approach, subgrid drag force, particle-particle collision

1. Introduction

Gas-solid reacting circulating fluidized beds are used in many industrial processes such as fluid catalytic cracking (FCC) in petroleum refineries or fossil combustion in power plants. Modelling of gas-particle flows, using the Two-Fluid Model (TFM) approach closed by the Kinetic Theory of Granular Flows (KTGF) is well established [3, 5, 11]. However, for A-type particles, according to Geldart's classification, the numerical simulations with coarse grids fail to predict the behaviour of the solid phase due to the inaccurate prediction of the solid clusters [2, 13, 14]. For instance, Parmentier et al. [14] shows that neglecting the small structures in dense fluidized bed simulation leads to an overestimation of the bed height. According to Ozel et al. [13] and Andreux et al. [1] the insufficient mesh refinement leads to underestimate the vertical solid mixing and residence time in circulating fluidized bed. In addition, in bi-solid circulating fluidized bed, Batrak et al. [3] show that the "coarse mesh" simulation leads to underestimate the momentum coupling between particle species with large density ratio and, consequently, the entrainment rate of the coarse particles by the small ones. The modelling strategy consists in splitting the local instantaneous variables in resolved and subgrid contributions. The corresponding governing equations are obtained by filtering the particle kinetic moment transport equations leading to unknown subgrid terms which need to be modelled in terms of the computed resolved variables. The first step is the budget analysis of the filtered transport equation and the evaluation of the resolved and subgrid contributions of each term. This step highlights which term(s) need(s) to be modelled, leading to the subgrid modelling step to account accurately for the effect of the small scale structures in the filtered equations. For monodisperse simulations, the drag force is overestimated by the resolved contribution and may lead to wrong predictions of the global hydrodynamic behaviour [15]. Several sub-grid models have been proposed by Ozel et al. [13], Parmentier et al. [15] to take into account the effect of the unpredicted solid cluster on filtered fluid-particle drag force modelling. For polydisperse simulations, the particle-particle mo-

mentum exchange has also to be studied. Holloway [6] focus on the need for sub-grid scale models for coarse-grid simulation of a binary gas-particle flow. The filtering of highly resolved simulation of bidisperse gas-particle flows shows that filtered constitutive relations also need to be developed for polydisperse systems to settle the difference between coarse grid and fine grid simulations. Ozel et al. [13] focus on the filtered momentum equation balance analysis in a bisolid fluidized bed, showing that subridmodels are needed for both the fluid-particle and particle-particle mean momentum transfer terms.

This article focus on the analysis of highly resolved simulations of bidisperse flow in a 3D periodic circulating fluidized bed. The resolved and unresolved contributions are compared for all the terms of the momentum and the kinetic agitation equations.

2. Mathematical modelling approach

The modelling approach is based on the Euler-Euler model, in which phases are treated as continuous interpenetrated media. The mass, the momentum and the energy Eulerian transport equations are solved for each phase and coupled by interphase transfer terms. The mass transport equation writes:

$$\frac{\partial}{\partial t}\alpha_k\rho_k + \frac{\partial}{\partial x_j}\rho_k\alpha_k U_{k,j} = 0. \tag{1}$$

with ρ_k the density of the kth phase and $U_{k,j}$ the jth component of the velocity.

The momentum transport equation writes:

$$\alpha_k\rho_k\left[\frac{\partial U_{k,i}}{\partial t} + U_{k,j}\frac{\partial U_{k,i}}{\partial x_j}\right] = \quad - \quad \alpha_k\frac{\partial P_g}{\partial x_i} + \alpha_k\rho_k g_i$$
$$+ \sum_{k'=g,p} I_{k'\to k,i} \tag{2}$$
$$- \frac{\partial \Sigma_{k,ij}}{\partial x_j} + \alpha_k F_{s,i}$$

In the equation 2, the first and second term on the right-hand-side are the pressure gradient, with P_g mean gas pressure, and the

gravity contributions with, g_i the ith component of the gravity, respectively. The third term on the right-hand-side represents the momentum transfer (without the mean gas pressure contribution). This term takes into account two mechanisms: the friction of the fluid on particles (gas $\leftrightarrow$ particles transfer) and the exchange of momentum by collisions (particles $\leftrightarrow$ particles transfer). The effective stress tensor has two components

$$\Sigma_{k,ij} = \alpha_k \rho_k \langle u'_{k,i} u'_{k,j} \rangle_p + \Theta_{k,ij} \tag{3}$$

where $\langle u'_{k,i} u'_{k,j} \rangle_p$ are the Reynolds stress tensor ($u'_{k,i}$ is the phase velocity fluctuation) and $\Theta_{k,ij}$ is the viscous stress tensor for the gas and the collisional stress tensor for particles. The term $F_{s,i}$ is a constant in the whole domain (as hereinafter defined). Hence, this term will not appear in the transport equation of the kinetic agitation q_p^2 and is independent of the filter width.

2.1. Gas-particle momentum transfer

The momentum transfer between gas and particles is done taking into account only the drag and Archimedes' pressure gradient force. Then, the fluid-particle transfer term in (2) is written:

$$I_{g \to p,i} = -\frac{\alpha_p \rho_p}{\tau_{fp}^F} (U_{p,i} - U_{g,i}) \tag{4}$$

The term satisfies $I_{g \to p,i} = -I_{p \to g,i}$. The particle relaxation timescale τ_{fp}^F is written as a function of the drag coefficient:

$$\frac{1}{\tau_{fp}^F} = \frac{3}{4} \frac{\rho_p}{\rho_g} \frac{\langle |v_r| \rangle_p}{d_p} C_d \tag{5}$$

The drag coefficient is calculated using the Wen and Yu correlation [17]. As Simonin et al. [16] show that the this model provides results close to the bidisperse LBM data and drag force correlations from the literature,

$$C_d = \frac{24}{Re_p}[1 + 0.15 Re_p^{0.687}]\alpha_g^{-1.7} \tag{6}$$

The particle Reynolds number is written as $Re_p = \frac{\alpha_g \rho_g \langle |v_r| \rangle d_p}{\mu_g}$.

2.2. Particle-particle momentum transfer

According to Gourdel et al. [4], the particle-particle momentum transfer term is written,

$$I_{p \to q,i} = \frac{m_p m_q}{m_p + m_q} \frac{1 + e_{pq}}{2} \frac{n_p}{\tau_{pq}^c} H_1(z)(U_{p,i} - U_{q,i}) \tag{7}$$

where m_p and m_q are the masses of particles p and q, e_{pq} the normal restitution coefficient of $p - q$ collision, τ_{pq}^c is characteristic time scale between two collisions of any p-particle with the q-particles and writes,

$$\frac{1}{\tau_{pq}^c} = g_0 n_q \pi d_{pq}^2 g_r \tag{8}$$

with d_{pq} the distance between particle centers when the collision takes place $d_{pq} = (d_p + d_q)/2$ and g_r the mean relative velocity of impact of particles of different types, written as:

$$g_r = \sqrt{\frac{16}{\pi} \frac{2}{3} q_r + V_{pq,i} V_{pq,i}} \tag{9}$$

$V_{pq,i}$ the relative velocity between particles is written: $V_{pq,i} = U_{p,i} - U_{q,i}$. q_r is the mean relative agitation of particles $q_r = \frac{1}{2}(q_p^2 + q_q^2)$ and g_0 the radial pair distribution function is calculated using [8],

$$g_0 = \left[1 - \frac{\alpha_s}{\alpha_{max}}\right]^{-2.5\alpha_{max}} \quad \text{if} \quad \alpha_s < \alpha_{max}^* \tag{10}$$

with α_s the whole solid volume fraction.

$H_1(z)$ is a function dealing with the change from a regime of collision controlled by the slip between particles to a regime controlled by the relative agitation which is approximated by [3],

$$H_1(z) = \frac{8 + 3z}{6 + 3z} \tag{11}$$

For $z \to 0$ the inter-species collisions are driven by the relative agitation. For $z \to +\infty$ the collisions are controlled by the mean particle-particle relative velocity.

$$z = \frac{V_{pq} V_{pq}}{\frac{8}{3} q_r} \tag{12}$$

2.3. Particle random kinetic energy modelling

The solid agitation is calculated using q_p^2 transport equation and viscosity model assumption developed in the frame of kinetic theory of polydisperse particle mixture accounting for the mean and fluctuant drag force effects [3, 11]:

$$\alpha_p \rho_p \left[\frac{\partial q_p^2}{\partial t} + U_{p,j} \frac{\partial q_p^2}{\partial x_j}\right] = \frac{\partial}{\partial x_j} \left[\alpha_p \rho_p (K_{p,kin} + K_{p,coll}) \frac{\partial q_p^2}{\partial x_j}\right]$$
$$+ \Pi_p + \epsilon_{fp}$$
$$+ \sum_q \epsilon_{pq} + \sum_q \chi_{pq} \tag{13}$$

In the Eqn.(13) the first term on the right-hand-side represents the kinetic diffusivity, the second term the energy production by velocity gradient,

$$\Pi_p = -\Sigma_{p,ij} \frac{\partial U_{p,i}}{\partial x_j} \tag{14}$$

The third term is the transfer of kinetic energy between gas and particle. It takes into account friction of the solid phase with the gas phase which is assumed to be laminar,

$$\epsilon_{fp} = -\frac{\alpha_p \rho_p}{\tau_{gp}^F} 2q_p^2 \tag{15}$$

The fourth term is the loss of energy due to inelastic collisions which is written:

$$\epsilon_{pq} = -m_p \left(\frac{2m_q}{m_p + m_q}\right)^2 \frac{1 - e_{pq}^2}{4} \frac{n_p}{\tau_{pq}^c} \frac{2}{3}(q_p^2 + q_q^2) \tag{16}$$

The last term is the transfer of kinetic energy between species and production by slip velocity between particles.

$$\chi_{pq} = P_{pq} + T_{pq} \tag{17}$$

$$P_{pq} = \frac{m_p m_q^2}{m_p + m_q} \frac{1 + e_{pq}}{4} \frac{n_p}{\tau_{pq}^c} |\mathbf{U}_p - \mathbf{U}_q|^2 H_1(z) \tag{18}$$

$$T_{pq} = -\frac{m_p m_q}{m_p + m_q} \frac{1 + e_{pq}}{2} \frac{n_p}{\tau_{pq}^c} \left[\frac{8}{3} \frac{m_p q_p^2 - m_q q_q^2}{m_p + m_q}\right] \tag{19}$$

3. Numerical simulation overview

Using the equations written below, several simulations of polydisperse and reactive flows were already conducted [7, 4]. Ozel et al. [12] highlighted effects of small structures on polydisperse simulations. In this study, gas-particles flows are simulated in a 3D periodical Circulating Fluidized Bed (CFB). The geometry, used previously by Ozel et al. [13], has a squared-section of 0.0275 m and a length of 0.22 m and is shown by Fig. 1.
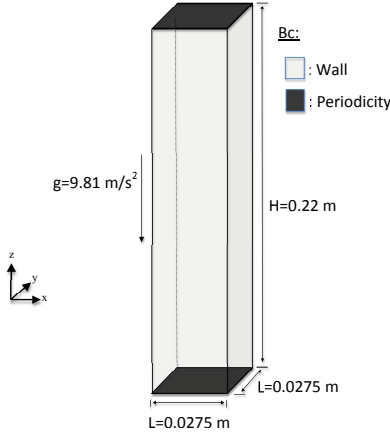

Figure 1: Sketch of the computational domain

Agrawal et al. [2] studied three different boundary conditions for the solid phase: free-slip, partial-slip (definition of a particle-wall restitution coefficient is needed) and no-slip. Meso-scale structures were observed in the three cases. In the case studied, the boundary conditions imposed at walls are no-slip for the gas and free-slip for the solid phase. Three meshes have been studied and the most refined mesh with a mesh size equal to $2.9 \cdot 10^{-3}$ m (about $7.1 \cdot 10^{6}$ mesh-cells) will be used for the budget analysis. For the case studied in the paper, the velocity fields are set initially to zero for all phases. The movement of the fluid is opposite to the gravity due to the pressure gradient imposed. The gas pressure is defined in a similar way than Agrawal et al. [2]. To ensure the periodicity of the simulation, it is necessary to maintain momentum in the whole domain at each time step. Considering the periodicity and the independence of $F_{s,i}$ from the filter width, the integration of the momentum equation 2 over the whole domain V is written as:

$$\frac{D\langle \alpha_k \rho_k W_k \rangle}{Dt} = \langle \alpha_k \rho_k g_z \rangle + \sum_{k'} \langle I_{k' \to k} \rangle + \langle \alpha_k \rangle F_{s,z} \quad (20)$$

where $\langle . \rangle$ is the domain-average operator. The sum of the Eqn. (20) for each phase gives the total momentum in the domain.

$$\frac{DM}{Dt} = \sum_k m_k g_z + F_{s,z} \quad (21)$$

with M is defined by $\sum \langle \alpha_k \rho_k W_k \rangle$ and m_k the total the total mass of phase k divided by the computational domain volume, independent of the time. One can write the equation in a discrete form with n is the actual time-step and $n + 1$ is the next time-step. We assume that this correction fulfils the flow condition where the total momentum at the next step, M^{n+1}, is equal to M^0. Then, the source term is

$$F_{s,z} = -\frac{M^n - M^0}{\Delta t} - \sum_k m_k g_z \quad (22)$$

For the case studied the materials properties are given in the Tab. 1:

Table 1: Particles and gas properties.

Prop.	Gas	Particle p	Particle q
$\rho \, [kg/m^3]$	1.186	1500	1500
$\mu \, [Pa \cdot s]$	$1.8 \cdot 10^{-5}$	-	-
$d_p \, [\mu m]$	-	75	150
$e_c \, [-]$	-	0.9	0.9
$\alpha_{p,ini} \, [m^3/m^3]$	0.90	0.05	0.05

Three dimensional numerical simulations of fluidized bed have been carried out using an Eulerian n-fluid modeling approach for gas-solid turbulent polydisperse flows developed and implemented by IMFT(Institut de Mécanique des Fluides de Toulouse. NEPTUNE_CFD is a multiphase flow software developed in the framework of the NEPTUNE project, financially supported by CEA (Commissariat à l'Energie Atomique), EDF (Electricité de France), IRSN (Institut de Radioprotection et de Sureté Nucléaire) and AREVA_NP. The numerical solver has been developed for High Performance Computing[9, 10].

4. Budget analysis of the filtered particulate momentum equation

Mesh independent results are used for the budget analysis of the filtered particle momentum and agitation equations. The aim of the analysis is to examine the contribution of sub-grid terms obtained after filtering equations. Different filter widths Δ have been applied to the results.The spatial filter applied is defined as:

$$G(\mathbf{x} - \mathbf{r}) = \left\{ \begin{array}{ll} \frac{1}{\Delta^3} & \max(x_i - r_i) \leq \frac{\Delta}{2} \\ 0 & \text{otherwise} \end{array} \right. \quad (23)$$

where G is a weight function which satisfies $\int \int \int G(\mathbf{r})d\mathbf{r} = 1$. The filtered phase volume fraction is defined as,

$$\tilde{\alpha}_k(\mathbf{x}, t) = \int \int \int \alpha_k(\mathbf{r}, t) G(\mathbf{x} - \mathbf{r})d\mathbf{r} \quad (24)$$

Filtered phase velocities are defined according to,

$$\tilde{U}_p(\mathbf{x}, t) = \frac{1}{\tilde{\alpha}_p} \int \int \int G(\mathbf{x} - \mathbf{r})\alpha_p(\mathbf{r}, t)U_p(\mathbf{r}, t)d\mathbf{r} \quad (25)$$

To obtain filtered values, especially solid volume fractions, independent of the filters widths, the domain studied is restricted to the interior of the periodic box and the regions near the walls are not taken into account, the distance between the wall and the domain taken studied is equal to $\delta = 0.1L$.

4.1. Particle momentum filtered transport equation

The filter is applied to the momentum equation (Eqn. (2)) and the filtered terms are decomposed into resolved and sub-grid terms. Additional terms arise in Eqn. (26) due to the filtering, the sub-grid contributions, noted f^{sgs}. After filtering and averaging each term over space and time, the momentum equation becomes:

$$\begin{aligned} \overline{\langle \tilde{\alpha}_p \rho_p \tilde{U}_{k,j} \frac{\partial \tilde{U}_{k,i}}{\partial x_j} \rangle} = &-\overline{\langle \tilde{\alpha}_p \frac{\partial \tilde{P}_g}{\partial x_i} \rangle} - \overline{\langle \varphi_{p,i}^{sgs} \rangle} + \overline{\langle \tilde{\alpha}_p \rho_p g_i \rangle} \\ &+ \overline{\langle \sum_{k'=g,p} I_{k' \to p,i}^{res.} \rangle} + \overline{\langle \sum_{k'=g,p} I_{k' \to p,i}^{sgs} \rangle} \\ &- \overline{\langle \frac{\partial}{\partial x_j} \Sigma_{p,ij}^{res} \rangle} - \overline{\langle \frac{\partial}{\partial x_j} \Sigma_{p,ij}^{sgs} \rangle} \\ &- \overline{\langle \frac{\partial}{\partial x_j} \rho_p \tilde{\alpha}_p \sigma_{p,ij}^{sgs} \rangle} \end{aligned}$$

$$(26)$$

The temporal averaged is represented by $\overline{f}$ and is done on 3.5s. f^{sgs} is defined as the difference between filtered and resolved contributions. A term calculated by using filtered values corresponds to a resolved contribution noted with the subscript f^{res}. For instance, $\varphi_{k,i}^{sgs}$ represents the sub-grid contribution of the correlation between fluctuations of the volume fractions of phases and gas pressure:

$$\varphi_{p,i}^{sgs} = \overline{\alpha_p \frac{\partial P_g}{\partial x_i}} - \tilde{\alpha}_p \frac{\partial \tilde{P}_g}{\partial x_i}. \tag{27}$$

The subgrid contributions of the particle kinetic stress, $\Sigma_{p,ij}^{sgs}$, the gas-particle momentum transfer, $I_{g \to p,i}^{sgs}$, and particle-particle momentum transfer, $I_{q \to p,i}^{sgs}$, are calculated similarly. The resolved gas-particle momentum transfer, particle-particle momentum transfer, pressure gradient contributions normalized by the gravity term are presented by Fig. 2 and 3 for small and large particles. For the small particles the main contribution is the drag force and for the large particles, it is the inter-particle momentum transfer. For both classes of particles, the resolved and sub-grid contributions can be neglected for the pressure gradient. Furthermore, the sub-grid gas-particle momentum transfer increases with the filter width, in agreement with the work of Ozel et al. [12]. The filtered gas-momentum transfer is overestimated by the resolved contribution and the subgrid contribution must be accounted for to correct this effect. The trend is similar for the particle-particle momentum transfer with an overestimation of the inter-species momentum transfer effect by the resolved contributions. So this effect should be accounted for by modelling the subgrid contribution. Therefore, this result may look in contradiction with coarse mesh simulation of bi-disperse gas-solid fluidized beds [3] where the inter-particle momentum transfer effects are underestimated. The probable explanation of this contradictory result is that the resolved collision frequency, and the corresponding momentum transfer, are underestimated due to a drastic underestimation of the resolved random particle kinetic energy in coarse mesh simulations. Then it is crucial to analyse the corresponding filtered equation to identify the missing contribution which should be accounted for to have a better prediction of the random particle kinetic energy. As for the pressure gradient, the sub-grid contributions of the kinetic stress and of the particle phase velocity fluctuations are negligible for both classes of particles.
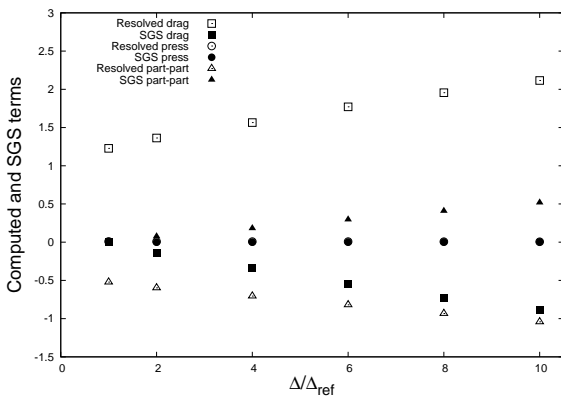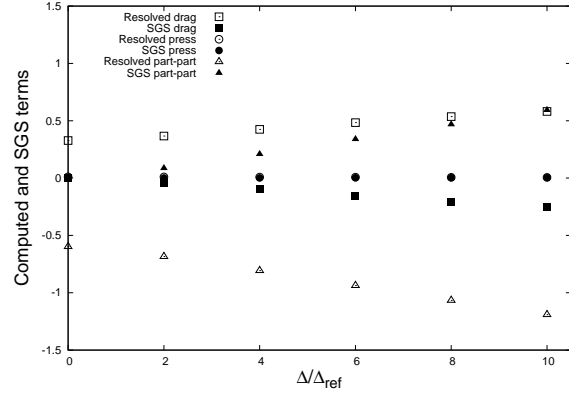

Figure 3: Resolved and sub-grid contributions in the particle momentum filtered transport equation for $d_p = 150\mu m$ for various filter widths Δ (normalized by $\tilde{\alpha}_q \rho_q g_z$)

4.2. Particle random kinetic energy filtered transport equation

The filtering process is applied to the random kinetic energy equation (13) to separate the resolved and the subgrid contributions. The filtered energy balance can be written as:

$$\overline{\langle \tilde{\alpha}_p \rho_p \tilde{U}_{k,j} \frac{\partial \tilde{q}_p^2}{\partial x_j} \rangle} = \overline{\langle \frac{\partial}{\partial x_j} \left[\tilde{\alpha}_p \rho_p \left(K_{p,kin}^{res} + K_{p,col}^{res} \right) \frac{\partial \tilde{q}_p^2}{\partial x_j} \right] \rangle}$$
$$+ \overline{\langle \frac{\partial}{\partial x_j} D_j^{sgs} \rangle} - \overline{\langle \Pi_p^{res} \rangle} - \overline{\langle \Pi_p^{sgs} \rangle}$$
$$- \overline{\langle \epsilon_{fp}^{res} \rangle} - \overline{\langle \epsilon_{fp}^{sgs} \rangle}$$
$$+ \overline{\langle \sum_q \epsilon_{pq}^{res} \rangle} + \overline{\langle \sum_q \epsilon_{pq}^{sgs} \rangle}$$
$$+ \overline{\langle \sum_q P_{pq}^{res} \rangle} + \overline{\langle \sum_q P_{pq}^{sgs} \rangle}$$
$$+ \overline{\langle \sum_q T_p^{res} \rangle} + \overline{\langle \sum_q T_p^{sgs} \rangle}$$
$$- \overline{\langle \frac{\partial}{\partial x_j} \alpha_p \rho_p Q_j^{sgs} \rangle}$$

$$\tag{28}$$

Figure 2: Resolved and sub-grid contributions in the particle momentum filtered transport equation for $d_p = 75\mu m$ for various filter widths Δ (normalized by $\tilde{\alpha}_p \rho_p g_z$)
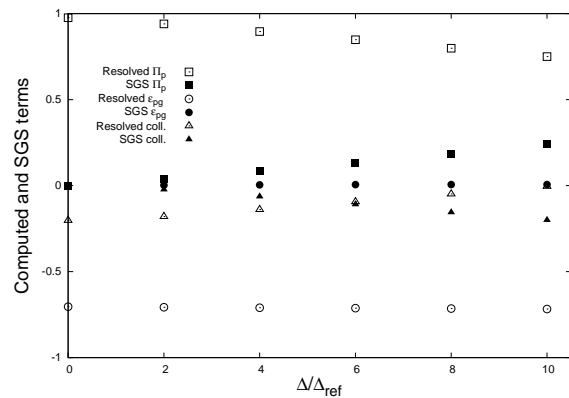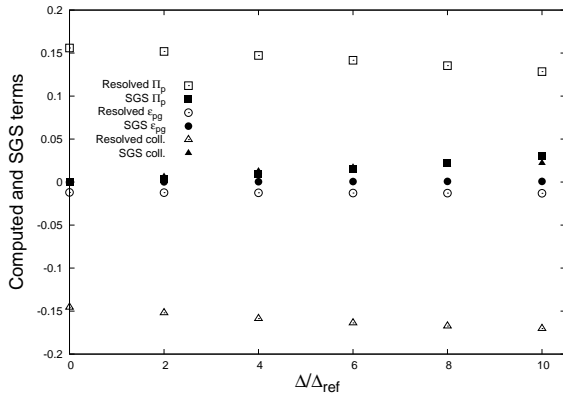

Figure 4: Resolved and sub-grid contributions in the random particle kinetic energy filtered transport equation for $d_p = 75\mu m$ for various filter widths Δ (normalized by $\tilde{\alpha}_p \rho_p V_{p,St}^2 / \tau_{p,St}$)

Figure 5: Resolved and sub-grid contributions in the random particle kinetic energy filtered transport equation for $d_p = 150\mu m$ for various filter widths Δ (normalized by $\tilde{\alpha}_q \rho_q V_{q,St}^2 / \tau_{q,St}$)
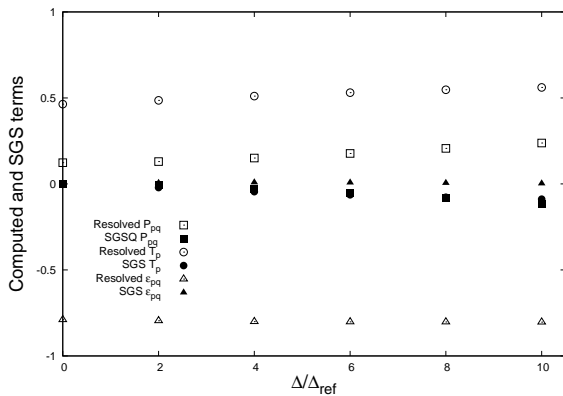

Figure 6: Resolved and sub-grid collision term contributions in the random particle kinetic energy filtered transport equation for $d_p = 75\mu m$ for various filter widths Δ (normalized by $\tilde{\alpha}_p \rho_p V_{p,St}^2 / \tau_{p,St}$)
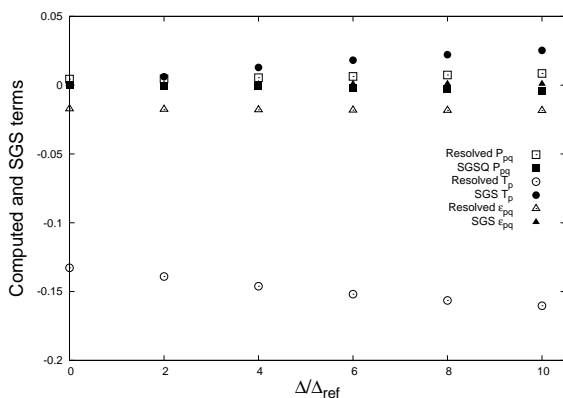

Figure 7: Resolved and sub-grid collision term contributions in the random particle kinetic energy filtered transport equation for $d_p = 150\mu m$ for various filter widths Δ (normalized by $\tilde{\alpha}_q \rho_q V_{q,St}^2 / \tau_{q,St}$)

The mean velocity and diffusive transport and the sub-grid particle kinetic energy flux are negligible compared to the others contributions and the study will focus on others contributions.

Figures 4 and 5 show the production by gradient, the dissipation by friction with the gas phase, the sum of all the contributions linked to collisions, the kinetic diffusivity according to the filter size. Figures 6 and 7 show the dissipation by inelastic collision, the production by relative velocity, the transfer by collisions as functions of the filter width. For the small particles, Figure 4 shows that the production by the mean velocity gradient is mostly in equilibrium with the dissipation by the fluid-particle drag and, secondarily, by inter-particle collision effects. The resolved production underestimates the filtered ones and should be completed by a subgrid contribution which increases with the filtered width. In contrast, the resolved collision term underestimates the filtered one while the subrid contribution to the dissipation by drag is negligible. Figure 6 shows the separate contributions of the collision terms with ϵ_{pq}, the inelastic dissipation, P_{pq}, the production by the mean relative particle motion, and T_p, the kinetic energy transfer between particle species. We can notice that the resolved kinetic energy transfer between particle species and the inelastic dissipation rate are nearly independent of the mesh size implying that the subgrid contributions are negligible. In contrast, the filtered production by the mean relative velocity between particle species is overestimated by the resolved one and the subgrid effect must be accounted for in the filtered modelling approach. Figure 5 shows that the budget of the coarse particle ($d_p = 150\mu m$) random filtered random kinetic energy equation is dominated by the equilibrium between mean velocity production and dissipation by the collision effect, while the drag dissipation effect looks nearly negligible. The resolved production is also decreasing with the filter width and the collision effect is overestimated by the resolved contribution. Figure 7 shows the separate contributions of the filtered collision term which confirms that the subgrid effect is measurable mostly for the production term due to the mean relative velocity between particle species.

5. Conclusion

Meso-scale structures are formed in the circulating fluidized bed and they can be resolved in the frame of Euler-Euler approach, based on kinetic theory of polydisperse granular flows, on high resolution computational grid. However, simulations with coarse meshes cannot account for these structures accurately and this may lead to very poor predictions of bed hydrodynamics for very small particle to mesh size ratio. For mono-dispersed gas-solid flow, Ozel et al. [13], and Parmentier et al. [14] analyse the effect of the small structures on the simulations for circulating fluidized bed and dense fluidised beds, respectively. In this study, we have investigated effects of unresolved structures on resolved field for gas-solid bidisperse flow. We first obtained mesh-independent results of gas-solid in a 3D periodic circulating fluidized bed. A filtering procedure was performed on particulate momentum and kinetic agitation equations. Additional resolved and subgrid terms appearing with the filtering procedure are investigated by budget analysis in order to identify the main sub-grid contributions. The analysis of the filtered momentum equation shows that the resolved fluid-particle drag and particle-particle collision are overestimating the momentum transfer effects and must be corrected by subgrid modelled contributions. The analysis of the budget of the filtered random kinetic energy shows that the resolved production by the mean shear and by the mean particle relative motion are overestimating the filtered ones. So new subgrid models have to be developed for these two terms while the subgrid contributions due to drag force or inelastic collision dissipations and to inter-particle redistribution are negligible.

6. Acknowledgements

References

[1] Andreux,R., Petit,G.,Hemati,M. and Simonin,O., Hydrodynamic and solid residence time distribution in a circulating fluidised bed: Experimental and 3D computational study, *Chemical Engineering and Processing:Process Intensification*, 47,463-473,2008.

[2] Agrawal, K., Holloway, Loezos, P. N., Syamal,M., Sundaresan, S., The role of meso-scale structures in rapid gas-solid flows, *Journal of Fluid Mechanics*, 445, 151-185, 2001.

[3] Batrak, O., Patino, G., Simonin, O., Flour, I., Le Guevel, T., Perez , E., Unlike Particles Size Collision Model in 3D Unsteady Polydispersed Simulation of Circulating Fluidised Bed, *Proceedings of the 8th Int. Conf. on Circulating Fluidized Beds*, In Circulating Fluidized Bed Technology VIII, Hangzhou (China), Kefa Cen (Ed.), 370-378, 2005.

[4] Fede, P., Simonin, O., Ghouila, I., 3D Numerical Simulation of Polydisperse Pressurized Gas-Solid Fluidized Bed, *Proceeding of AJK2011-FED,* , ASME-JSME-KSME Joint Fluids Engineering Conference 2011, Hamamatsu, Shizuoka (Japan), AJK2011-12016, 2011.

[5] Gourdel, C., Simonin, O., Brunier, E., Two-Maxwellian Equilibrium Distribution Function for the Modelling of a Binary Mixture of Particles, *Circulating Fluidized Bed Technology VI, Proc. of the 6th Int. Conference on Circulating Fluidized Beds*, Werther (Editor), DECHEMA, Frankfurt am Main (Germany), 205-210, 1999.

[6] Holloway,W., Benyahia, S., Hrenya, C.M., Sundaresan, S., Meso-scale structures of bidisperse mixtures of particles fluidized by a gas, *Chemical Engineering Science*, 66, 4403-4420, 2011.

[7] Konan, N.A., Neau, H., Simonin, O., Dupoizat, M., Le Goaziou, T., Reactive multiphase flow simulation of uranium hexafluoride conversion reactor   *7th International Conference on Multiphase Flow*, Tampa,2010.

[8] Lun,C. K. K., Savage, S. B., The effects of an impact velocity depedent coefficient of restitution coefficient of restitution on stesses developed by sheared granular materials, *Acta Mechanicas*, 63, 15-44, 1986.

[9] Neau, H., Laviéville, J., Simonin, O., NEPTUNE_CFD High parallel Computing Performance for Particle-Laden Reactive Flows, *7th International Conference on Multiphase Flow*, Tampa , 2010.

[10] Neau, H., Fede, P., Laviéville, J. and Simonin, O. High Performance Computing (HPC) for the Fluidization of Particle-Laden Reactive Flows, *The 14th International Conference on Fluidization - From Fundamentals to Products*, 2013.

[11] Nouyrigat N., Bousquet E., Simonin O., Lalam V., 2011, A Numerical and Experimental Study of Hydrodynamic Behavior of Bisolid Circulatin g Fluidized Beds, *8th International Conference on CFD in Oil & Gas, Metallurgical and Process Industries*, Trondheim (Norway), 2011.

[12] Ozel, A., Fede, P., Simonin, O. Effect of unresolved structures on the Euler-Euler simulation of 3D periodic circulating fluidized of binary mixture, *8th International Conference on Multiphase Flow*, 2013.

[13] Ozel, A., Fede, P., Simonin, O. Development of filtered Euler-Euler two-phase model for circulating fluidized bed: high resolution simulation, formulation and a Priori analyses, *Int. J. Multiphase Flow*, Vol. 55, pp. 43-63, 2013.

[14] Parmentier, J.F., Simonin, O., Delsart, O., A Numerical Study of Fluidization Behaviour of Geldart B, A/B and A Particles Using an Eulerian Multifluid Modeling Approach, *Proc. of the 9th Int. Conference on Circulating Fluidized Beds*, Circulating Fluidized Bed Technology IX, Werther & al. (Editors), Hamburg (Germany), pp 331-336, 2008.

[15] Parmentier, J.F., Simonin, O., Delsart, O., A functional subgrid drift velocity model for filtered drag prediction in dense fluidized bed, *AIChE Journal*, Vol. 58, Issue 4, pp. 1084-1098, 2012.

[16] Simonin, O., Chevrier, S., Audard, F., Fede, P., Drag force modelling in dilute to dense particle-laden flows with monodisperse or binary mixture of solid particles, *Proc. of the 9th International Conference on Multiphase Flow*, Firenze (Italy),2016.

[17] Wen, Y., Yu, Y., Mechanics of fluidization. *Chemical Engineering Symposium*, Series 62, 100-111, 1965.